Title

STOCHASTIC RESPONSE QUANTIFICATION OF FIXED-BASE AND BASE-ISOLATED RIGID-PLASTIC BLOCKS

ISBN

9786188284494

Authors

Kasinos, Stavros

Ma, Fai

Publication Date

2019

DOI

10.7712/120219.6325.18726

Peer reviewed

UNCECOMP 2019
3rd ECCOMAS Thematic Conference on
Uncertainty Quantification in Computational Sciences and Engineering
M. Papadrakakis, V. Papadopoulos, G. Stefanou (eds.)
Crete, Greece, 24—26 June 2019

STOCHASTIC RESPONSE QUANTIFICATION OF FIXED-BASE AND BASE-ISOLATED RIGID-PLASTIC BLOCKS

Stavros Kasinos[1] **and Fai Ma**[2]

[1]Imperial College London
Department of Aeronautics, SW7 2AZ, London, UK
e-mail: s.kasinos@imperial.ac.uk

[2] University of California, Berkeley
Department of Mechanical Engineering, California 94720-1740, US
e-mail: fma@berkeley.edu

Keywords: Base Isolation, Earthquake, Rigid-plastic, Sliding, Statistical Linearisation, Stochastic Excitation.

Abstract. *The paper deals with the modelling, response quantification and vibration control of rigid-plastic blocks in presence of stochastic forcing with indicative application to seismic engineering. The full dynamic interaction between a rigid-plastic block and a linear base-isolation system is considered and efficient piecewise numerical solutions are derived for analysing the true nonlinear response, in comparison with the base-fixed counterpart. Stochastic forcing is modelled as stationary filtered white noise, characterised by a modified version of the Kanai-Tajimi power spectrum suggested by Clough and Penzien, commonly used in earthquake engineering applications. A statistical linearisation approach is adopted in view of approximating the strongly nonlinear systems during the sliding motion regime, which conveniently permits quantification of the steady-state, stationary response statistics. The accuracy of the linearisation approximation is investigated, and the effectiveness of the base isolation in suppressing the extreme forcing delivered to the block is assessed. The work delivers insights into the determination and understanding of the probabilistic characteristics of the response of dynamically driven base-fixed and base-isolated rigid-plastic systems, further encouraging investigations on other types of structures, isolation systems and hazard scenarios.*

1 INTRODUCTION

For the vast majority of the structural systems encountered in engineering, it is of paramount importance to understand the dynamics that underpin their response and reliability in the occurrence of extreme environmental loading conditions. Examples include motions of high speed crafts and ships in rough seas [1], vibration of buildings and offshore structures due to wave impacts [2], wind loads [3] and earthquakes [4]. It is widely common to cast idealised models for these structures or their subsystems, as a starting point in characterising their behaviour. The class of *block-type* models, for instance, can be considered representative of the *acceleration-sensitive rigid systems*, that is, a broad spectrum of the mechanical, electrical and electronic equipment of engineering interest (e.g. transformers, emergency generators, computer cabinets, compressors, medical and telecommunications equipment etc.) whose survivability and operational continuity during transportation and throughout their design life is critical. Inherent nonlinearities and uncertainties in their properties, the presence of randomness in the external excitation as well as the type of hazard, pose challenges that render the determination of their response statistics as a non-straightforward task.

Of interest is the case of the idealised sliding block, exhibiting rigid-plastic behaviour, a widely accepted model representing a broad range of structural and geotechnical systems, including buildings on moving foundation, equipment, retaining walls, slopes and masonry. Several studies have been devoted to the deterministic seismic analysis of such blocks, including those dealing with idealised ground acceleration pulses [5–7] and recorded earthquake ground motions [8]. The stochastic response of such systems has been examined in presence of white noise [9] and filtered white noise, characterised by the Kanai-Tajimi [10, 11] power spectrum [12–17], mostly for applications dealing with rigid structures resting on a frictional foundation. Modelling the excitation as white noise, however, implies infinite power of the resulting process, which is unphysical. Nonetheless, such idealisation can deliver useful insights in analysis, provided the results are carefully interpreted. The Kanai-Tajimi spectrum on the other hand, provides a more realistic model for earthquake engineering applications, however, it has been criticised due to the presence of low-frequency content [18].

Among risk mitigation technologies, base isolation aims at limiting the vibration response of the system to be controlled via the use of supports that uncouple the structure from the ground. Theory and practice are covered in several books and papers; a comprehensive review of the subject is given by Kelly [19]. Previous endeavours in this context investigate the effectiveness of seismic isolation on the primary load-bearing structure [20], with limited efforts to examine such effects on the performance of components. The 'cascade' response of rigid-plastic systems, for instance, has been examined in base-isolated buildings subjected to broadband ground motions [21, 22]. Adequate characterisation of the nonlinear dynamics for the combined primary-secondary system assembly is in fact necessary, when the equipment vibrates close to, or is tuned with the primary structure. From a different viewpoint, isolation directly applied on the component can be a viable cost-effective strategy to protect sensitive equipment in critical facilities [19]. Nevertheless, to our knowledge, the only past publication dealing with isolation directly on the sliding component is the one by Roussis *et al*. [23], which tackles the problem on a conventional deterministic basis.

Recognising the importance of understanding the response probabilistic characteristics of such systems, this paper addresses the modelling, response quantification and vibration control of rigid-plastic blocks, in presence of stochastic forcing with indicative application to seismic engineering. The scope of the paper is fivefold: (1) to characterise the full dynamic interaction

between a rigid-plastic block and a linear base-isolation system; (2) to derive efficient piece-wise numerical solutions for quantifying the nonlinear response of fixed-base and base-isolated rigid-plastic blocks to a general-type excitation; (3) to quantify the statistics of the steady-state, stationary response of the associated equivalent linear systems during the sliding motion regime, in presence of excitation characterised by the Clough-Penzien spectrum; (4) to investigate the acuracy of the linearisation approximation; and (5) to assess the effectiveness of the isolation in suppressing the seismic forcing delivered to the block. The work will form the basis for extending our investigations to other types of systems and hazard scenarios.

2 VIBRATION OF FIXED-BASE AND BASE-ISOLATED RIGID-PLASTIC BLOCKS

2.1 Fixed-base rigid-plastic block

Let us consider first the case of a rigid-perfectly plastic single-degree-of-freedom (SDoF) block (S), as depicted in Figure 1(a). The block has a mass m_s and is subjected to the horizontal base acceleration $\ddot{\xi}(t)$, where the overdot denotes differentiation with respect to time and $u_\mathrm{s}(t)$ is the unidirectional displacement, relative to the ground.

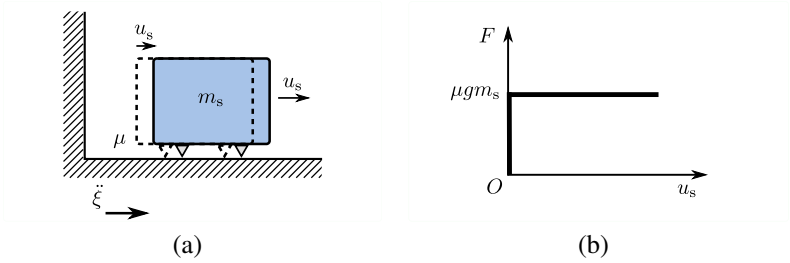

Figure 1: Free-standing sliding block (a) and force-displacement relationship (b).

The system exhibits infinite pre-yielding stiffness and infinite ductility, and the restoring force takes the form:

$$f_s = \begin{cases} \in [-\mu\, g\, m_\mathrm{s}, \mu\, g\, m_\mathrm{s}]\,, & \dot{u}_\mathrm{s} = 0 \\ \mu\, g\, m_\mathrm{s}\, \mathrm{sgn}\left(\dot{u}_\mathrm{s}(t)\right), & \text{otherwise} \end{cases}, \tag{1}$$

in which $\mu = a_\mathrm{s}/g$ is the coefficient of sliding friction assuming horizontal contact surface, a_s being the system's specific strength (i.e. the level of the ground acceleration $\ddot{\xi}(t)$ required for S to yield), and g is the acceleration due to gravity; $\mathrm{sgn}(\bullet)$ denotes the signum function (i.e. $\mathrm{sgn}(x) = +1$ if $x > 0$, $\mathrm{sgn}(x) = -1$ if $x < 0$, and $\mathrm{sgn}(x) = 0$ if $x = 0$). Evidently, the formalism given by Eq. (1) contains information about two distinct motion regimes, namely, sticking (i.e. when $\dot{u}_\mathrm{s} = 0$), and slipping [24].

The equation of motion for S is:

$$\ddot{u}_\mathrm{s}(t) = \begin{cases} 0, & u_\mathrm{s}, \dot{u}_\mathrm{s} = 0 \\ -\mu\, g\, \mathrm{sgn}\left(\dot{u}_\mathrm{s}(t)\right) - \ddot{\xi}(t), & \text{otherwise} \end{cases}. \tag{2}$$

The initiation condition for the sliding regime is set to $|\ddot{\xi}(t)| = \mu\, g$ (Figure 1(b)). Following initiation, an instantaneous stop or a full stop can occur in the system once the velocity drops to zero ($\dot{u}_\mathrm{s} = 0$). In the former case, the motion will reverse or it will continue in the same direction, while in the latter case the system will remain at rest until the initiation condition is exceeded again.

2.2 Base-isolated rigid-plastic block

Consider now the case of a two-degree-of-freedom (TDoF) system, comprising of the block S being supported on a linear base isolation system (B) undergoing horizontal accelerated motion, as depicted in Figure 2(a), where $u_\mathrm{b}(t)$, $u_\mathrm{s}(t)$ are the unidirectional displacements of B and S, relative to the ground, and $u_\mathrm{s}^\mathrm{b}(t) = u_\mathrm{s}(t) - u_\mathrm{b}(t)$ is the motion of S relative to B.

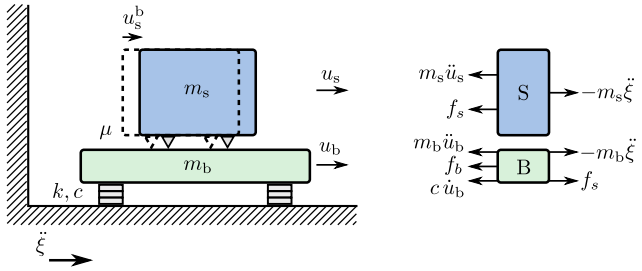

(a) (b)

Figure 2: TDoF system: sliding block on a linear isolation system (a); free-body diagram (b).

Figure 2(b) shows the forces acting on B and S, where m_b and m_s are the associated masses. Further extending the formulation in [4], $f_b(t) = \omega_\mathrm{b}^2\, m_\mathrm{b}\, u_\mathrm{b}(t)$ represents the restoring force in B, where $\omega_\mathrm{b} = \sqrt{k/m_\mathrm{t}}$ is the associated natural circular frequency, k being the stiffness of a linear spring and $m_\mathrm{t} = m_\mathrm{b} + m_\mathrm{s}$ the total mass of the system. Furthermore, $c = 2\,\zeta\omega_\mathrm{b}\, m_\mathrm{t}$ is the viscous damping coefficient, where ζ is the equivalent viscous damping ratio. The rigid-perfectly plastic S system finally assumes a restoring force, f_s as in Eq. (1), where $\dot{u}_\mathrm{s}^\mathrm{b}$ is used in place of $\dot{u}_\mathrm{s}$.

Dynamic equilibrium of the mass m_p in the horizontal direction then gives:

$$\ddot{u}_\mathrm{b}(t) = -\gamma\,\ddot{u}_\mathrm{s}^\mathrm{b}(t) - 2\,\zeta\omega_\mathrm{b}\,\dot{u}_\mathrm{b}(t) - \omega_\mathrm{b}^2\,u_\mathrm{b}(t) - \ddot{\xi}(t)\,; \quad u_\mathrm{b}(0) = \dot{u}_\mathrm{b}(0) = 0\,, \tag{3}$$

where $\gamma = m_\mathrm{s}/m_\mathrm{t}$ is the ratio of the block's mass to the total mass of the system, controlling the relative significance of the feedback action on B.

Setting $u_\mathrm{s}^\mathrm{b}(t) = \dot{u}_\mathrm{s}^\mathrm{b}(t) = 0$ in the above for the sticking phase where no relative motion is exhibited for S, the resulting system can be interpreted as an equivalent oscillator with mass m_t.

Equilibrium of the forces (Figure 2(b)) gives the equation of motion for S:

$$\ddot{u}_\mathrm{s}^\mathrm{b}(t) = \begin{cases} 0, & u_\mathrm{s}^\mathrm{b},\, \dot{u}_\mathrm{s}^\mathrm{b} = 0 \\ -\mu\, g\, \mathrm{sgn}\left(\dot{u}_\mathrm{s}^\mathrm{b}(t)\right) - \ddot{u}_\mathrm{b}(t) - \ddot{\xi}(t), & \text{otherwise} \end{cases}. \tag{4}$$

The initiation condition for sliding in the TDoF system is set to $|\ddot{u}_\mathrm{b}(t) + \ddot{\xi}(t)| = \mu\, g$, $\ddot{u}_\mathrm{b}(t)$ being a solution of Eq. (3).

Equations (3) and (4) are cast in a state space form (i.e. explicit expressions of the state variables) and are solved together. In this case, the state vector is:

$$\mathbf{y}\,(t) = \begin{cases} \left\{ u_\mathrm{b}(t) \,\vdots\, \dot{u}_\mathrm{b}(t) \right\}^\top, & u_\mathrm{s}^\mathrm{b},\, \dot{u}_\mathrm{s}^\mathrm{b} = 0 \\ \left\{ u_\mathrm{s}^\mathrm{b}(t) \,\vdots\, \dot{u}_\mathrm{s}^\mathrm{b}(t) \,\vdots\, u_\mathrm{b}(t) \,\vdots\, \dot{u}_\mathrm{b}(t) \right\}^\top, & \text{otherwise} \end{cases}, \tag{5}$$

whose time derivative is:

$$\dot{\mathbf{y}}\left(t\right)=\left\{\begin{array}{l}\left\{\begin{array}{c}\dot{u}_{\mathrm{b}}(t)\\ -2\,\zeta\,\omega_{\mathrm{b}}\dot{u}_{\mathrm{b}}(t)-\omega_{\mathrm{b}}^{2}u_{\mathrm{b}}(t)-\ddot{\xi}(t)\end{array}\right\}, \quad u_{\mathrm{s}}^{\mathrm{b}},\dot{u}_{\mathrm{s}}^{\mathrm{b}}=0\\ \left\{\begin{array}{c}\dot{u}_{\mathrm{s}}^{\mathrm{b}}(t)\\ \frac{-\mu\,g\,\mathrm{sgn}\left(\dot{u}_{\mathrm{s}}^{\mathrm{b}}(t)\right)+2\,\zeta\omega_{\mathrm{b}}\dot{u}_{\mathrm{b}}(t)+\omega_{\mathrm{b}}^{2}u_{\mathrm{b}}(t)}{1-\gamma}\\ \dot{u}_{\mathrm{b}}(t)\\ \frac{\gamma\,\mu\,g\,\mathrm{sgn}\left(\dot{u}_{\mathrm{s}}^{\mathrm{b}}(t)\right)-2\,\zeta\omega_{\mathrm{b}}\dot{u}_{\mathrm{b}}(t)-\omega_{\mathrm{b}}^{2}u_{\mathrm{b}}(t)}{1-\gamma}-\ddot{\xi}(t)\end{array}\right\}, \quad \text{otherwise}\end{array}\right. . \tag{6}$$

During the sticking phase, integration is carried out solely for B based on the top part of Eq. (6), using the initial conditions from the last step. Following initiation integration proceeds thereafter using the bottom part of the equation.

It is worth mentioning that the formulation presented herein, is in agreement with an equivalent expression in [23] for the sliding motion regime, and delivers further insights during the sticking motion regime.

3 NUMERICAL PROCEDURE FOR PIECEWISE RESPONSE QUANTIFICATION

Owing to the piecewise linear form of the dynamical systems considered, a highly efficient numerical procedure is employed for quantifying the true nonlinear response due to a general-type of excitation. In what follows, each regime of motion is separately considered and the response time history is constructed by piecing together the individual segments.

3.1 Fixed-base rigid-plastic block

The response of the SDoF system in Eq. (2) is considered first during the sliding motion regime. Accordingly, a numerical scheme [4] is adopted for the response evaluation by interpolating the excitation over each time interval. The response vector is then readily determined through the recurrence formula:

$$\mathbf{y}(t_{i+1})=\begin{bmatrix}1 & \Delta t\\ 0 & 1\end{bmatrix}\cdot\mathbf{y}(t_i)-\begin{bmatrix}\frac{\Delta t^2}{3}\\ \frac{\Delta t}{2}\end{bmatrix}\cdot\eta(t_i)-\begin{bmatrix}\frac{\Delta t^2}{6}\\ \frac{\Delta t}{2}\end{bmatrix}\cdot\eta(t_{i+1})\,, \tag{7}$$

where $\mathbf{y}(t)=\{u_{\mathrm{s}}(t),\dot{u}_{\mathrm{s}}(t)\}^{\top}$ and $\eta\left(t\right)=\ddot{\xi}(t)+\mu\,g\,\mathrm{sgn}\left(\dot{u}_{\mathrm{s}}(t)\right)$. Notably, the only restriction in Eq. (7) is that Δt is sufficiently low to closely approximate the excitation.

3.2 Base-isolated rigid-plastic block

The TDoF system in Eq. (6) is considered next. Similar to the fixed-base block, the response is separately derived for the sticking and sliding motion regimes. The response vector is then obtained from the recurrence formula:

$$\mathbf{y}(t_{i+1})=\boldsymbol{\Theta}(\Delta t)\cdot\mathbf{y}(t_i)+\boldsymbol{\Gamma}_0(\Delta t)\cdot\mu\,g\,\mathrm{sgn}\left(\dot{u}_{\mathrm{s}}^{\mathrm{b}}(t)\right)+\boldsymbol{\Gamma}_1(\Delta t)\cdot\ddot{\xi}\left(t_i\right)+\boldsymbol{\Gamma}_2(\Delta t)\cdot\ddot{\xi}\left(t_{i+1}\right)\,, \tag{8}$$

where $\boldsymbol{\Theta}(\Delta t)$ is the so-called transition matrix, and $\boldsymbol{\Gamma}_0(\Delta t)$, $\boldsymbol{\Gamma}_1(\Delta t)$ and $\boldsymbol{\Gamma}_2(\Delta t)$ are vectors depending on Δt, which is tacitly assumed sufficiently small so that the interpolation of the force is satisfactory.

During the sticking regime, $\mathbf{\Theta}(\Delta t)$ is given by:

$$\mathbf{\Theta}(\Delta t) = \begin{bmatrix} \mathcal{A}(\Delta t) & \mathcal{B}(\Delta t) \\ -\omega_{\mathrm{b}}^2\,\mathcal{B}(\Delta t) & \mathcal{A}(\Delta t) - 2\,\zeta\omega_{\mathrm{b}}\mathcal{B}(\Delta t) \end{bmatrix}, \tag{9}$$

where $\mathcal{A}(\Delta t) = e^{-\zeta\omega_{\mathrm{b}}\Delta t}\cos(\omega_{\mathrm{d}}\Delta t) + \zeta\omega_{\mathrm{b}}\,\mathcal{B}(\Delta t)$, $\mathcal{B}(\Delta t) = \frac{e^{-\zeta\omega_{\mathrm{b}}\Delta t}}{\omega_{\mathrm{d}}}\sin(\omega_{\mathrm{d}}\Delta t)$, and $\omega_{\mathrm{d}} = \omega_{\mathrm{b}}\sqrt{1-\zeta^2}$ is the damped circular frequency.

Furthermore, $\mathbf{\Gamma}_0(\Delta t)$ is a zero vector and $\mathbf{\Gamma}_1(\Delta t)$, $\mathbf{\Gamma}_2(\Delta t)$ are given by:

$$\mathbf{\Gamma}_1(\Delta t) = \begin{bmatrix} \frac{\omega_{\mathrm{b}}\Delta t\mathcal{A}(\Delta t)+2\,\zeta(\mathcal{A}(\Delta t)-1)-\omega_{\mathrm{b}}\mathcal{B}(\Delta t)}{\omega_{\mathrm{b}}^3\Delta t} \\ \frac{1-\mathcal{A}(\Delta t)}{\omega_{\mathrm{b}}^2\Delta t} - \mathcal{B}(\Delta t) \end{bmatrix}; \tag{10}$$

$$\mathbf{\Gamma}_2(\Delta t) = \begin{bmatrix} \frac{-2\,\zeta\mathcal{A}(\Delta t)+\omega_{\mathrm{b}}\mathcal{B}(\Delta t)-\omega_{\mathrm{b}}\Delta t+2\,\zeta}{\omega_{\mathrm{b}}^3\Delta t} \\ \frac{\mathcal{A}(\Delta t)-1}{\omega_{\mathrm{b}}^2\Delta t} \end{bmatrix}. \tag{11}$$

For the sliding regime, the response depends on:

$$\mathbf{\Theta}(\Delta t) = \begin{bmatrix} 1 & \Delta t & 1-\zeta\omega_{\mathrm{b}}\,\mathbb{F}-\omega_{\mathrm{d1}}\mathbb{Q} & \Delta t+(\gamma-1)\mathbb{F} \\ 0 & 1 & \omega_{\mathrm{b}}^2\,\mathbb{F} & 1+\zeta\omega_{\mathrm{b}}\,\mathbb{F}-\omega_{\mathrm{d1}}\mathbb{Q} \\ 0 & 0 & \zeta\omega_{\mathrm{b}}\,\mathbb{F}+\omega_{\mathrm{d1}}\mathbb{Q} & (1-\gamma)\mathbb{F} \\ 0 & 0 & -\omega_{\mathrm{b}}^2\,\mathbb{F} & \omega_{\mathrm{d1}}\mathbb{Q}-\zeta\omega_{\mathrm{b}}\,\mathbb{F} \end{bmatrix}; \tag{12}$$

$$\mathbf{\Gamma}_0(\Delta t) = \begin{bmatrix} \frac{\gamma(\zeta\omega_{\mathrm{b}}\,\mathbb{F}+\omega_{\mathrm{d1}}\mathbb{Q}-1)}{\omega_{\mathrm{b}}^2} - \frac{\Delta t^2}{2} \\ -\gamma\,\mathbb{F}-\Delta t \\ -\frac{\gamma(\zeta\omega_{\mathrm{b}}\,\mathbb{F}+\omega_{\mathrm{d1}}\mathbb{Q}-1)}{\omega_{\mathrm{b}}^2} \\ \gamma\,\mathbb{F} \end{bmatrix}; \tag{13}$$

$$\mathbf{\Gamma}_1(\Delta t) = \begin{bmatrix} \frac{6(\gamma-1)\zeta^2\mathbb{F}\omega_{\mathrm{b}}+\omega_{\mathrm{b}}\left(\Delta t^3\left(-\omega_{\mathrm{b}}^2\right)+3(\gamma-1)^2\mathbb{F}+3(\gamma-1)\Delta t\mathbb{Q}\omega_{\mathrm{d1}}\right)+3(\gamma-1)\zeta\left(\Delta t\mathbb{F}\omega_{\mathrm{b}}^2+2\mathbb{Q}\omega_{\mathrm{d1}}-2\right)}{3\Delta t\omega_{\mathrm{b}}^3} \\ -\frac{\Delta t^2\omega_{\mathrm{b}}^2-2\mathbb{F}\omega_{\mathrm{b}}(\Delta t\omega_{\mathrm{b}}+\zeta)+2\gamma(\mathbb{F}\omega_{\mathrm{b}}(\Delta t\omega_{\mathrm{b}}+\zeta)+\mathbb{Q}\omega_{\mathrm{d1}}-1)-2\mathbb{Q}\omega_{\mathrm{d1}}+2}{2\Delta t\omega_{\mathrm{b}}^2} \\ -\frac{(\gamma-1)((\gamma-1)\mathbb{F}\omega_{\mathrm{b}}+\zeta(\mathbb{F}\omega_{\mathrm{b}}(\Delta t\omega_{\mathrm{b}}+2\zeta)-2)+\mathbb{Q}\omega_{\mathrm{d1}}(\Delta t\omega_{\mathrm{b}}+2\zeta))}{\Delta t\omega_{\mathrm{b}}^3} \\ \frac{(\gamma-1)(\mathbb{F}\omega_{\mathrm{b}}(\Delta t\omega_{\mathrm{b}}+\zeta)+\mathbb{Q}\omega_{\mathrm{d1}}-1)}{\Delta t\omega_{\mathrm{b}}^2} \end{bmatrix}; \tag{14}$$

$$\mathbf{\Gamma}_2(\Delta t) = \begin{bmatrix} -\frac{\Delta t^3\omega_{\mathrm{b}}^3+6(\gamma-1)\omega_{\mathrm{b}}(\Delta t+(\gamma-1)\mathbb{F})+12(\gamma-1)\zeta^2\mathbb{F}\omega_{\mathrm{b}}+12(\gamma-1)\zeta(\mathbb{Q}\omega_{\mathrm{d1}}-1)}{6\Delta t\omega_{\mathrm{b}}^3} \\ -\frac{\Delta t^2\omega_{\mathrm{b}}^2+2\zeta\mathbb{F}\omega_{\mathrm{b}}-2\gamma(\zeta\mathbb{F}\omega_{\mathrm{b}}+\mathbb{Q}\omega_{\mathrm{d1}}-1)+2\mathbb{Q}\omega_{\mathrm{d1}}-2}{2\Delta t\omega_{\mathrm{b}}^2} \\ \frac{(\gamma-1)(\omega_{\mathrm{b}}(\Delta t+(\gamma-1)\mathbb{F})+2\zeta(\zeta\mathbb{F}\omega_{\mathrm{b}}+\mathbb{Q}\omega_{\mathrm{d1}}-1))}{\Delta t\omega_{\mathrm{b}}^3} \\ -\frac{(\gamma-1)(\zeta\mathbb{F}\omega_{\mathrm{b}}+\mathbb{Q}\omega_{\mathrm{d1}}-1)}{\Delta t\omega_{\mathrm{b}}^2} \end{bmatrix}, \tag{15}$$

where the above depend on $\mathbb{F}(\Delta t) = \frac{1}{\omega_{\mathrm{d1}}}e^{\frac{\zeta\omega_{\mathrm{b}}\Delta t}{\gamma-1}}\sin(\frac{\omega_{\mathrm{d1}}\Delta t}{1-\gamma})$, $\mathbb{Q}(\Delta t) = \frac{1}{\omega_{\mathrm{d1}}}e^{\frac{\zeta\omega_{\mathrm{b}}\Delta t}{\gamma-1}}\cos(\frac{\omega_{\mathrm{d1}}\Delta t}{1-\gamma})$ and $\omega_{\mathrm{d1}} = \omega_{\mathrm{b}}\sqrt{1-\gamma-\zeta^2}$.

In using the piecewise linear solutions presented herein, the response is evaluated separately during the sticking and sliding motion regimes and once both components have been determined the overall response is constructed by piecing together the individual segments. Notably, an iterative scheme needs to be employed to identify the time of initiation for each regime of motion as well as subsequent changes in the regime when the velocity changes sign. Details on the numerical implementation procedure are provided in Appendix A.

4 STOCHASTIC MODEL OF SEISMIC FORCING

Let us now consider a ground acceleration $\ddot{\xi}(t)$, modelled as stationary filtered white noise process, characterised by a more realistic version of the Kanai-Tajimi power spectrum [10, 11], suggested by Clough and Penzien [25], commonly used in earthquake engineering applications.

The spectral density function takes the form:

$$S_{\ddot{\xi}}(\omega) = S_0 \cdot H_k(\omega) \cdot H_c(\omega)\,; \quad -\infty < \omega < \infty\,, \tag{16}$$

where S_0 represents a constant power spectral density level due to white noise, $H_k(\omega)$ and $H_c(\omega)$ represent the Kanai-Tajimi and Clough-Penzien filters, respectively, given by:

$$H_k(\omega) = \frac{1 + 4\,\zeta_g^2\,(\omega/\omega_g)^2}{\left(1 - (\omega/\omega_g)^2\right)^2 + 4\,\zeta_g^2\,(\omega/\omega_g)^2}\,; \quad H_c(\omega) = \frac{(\omega/\omega_f)^4}{\left(1 - (\omega/\omega_f)^2\right)^2 + 4\,\zeta_f^2\,(\omega/\omega_f)^2}\,, \tag{17}$$

where the parameters ω_g and ζ_g denote the frequency and damping ratio of the soil layer, respectively, and ω_f, ζ_f control the Clough-Penzien filter's characteristics.

In this model, the first filter $H_k(\omega)$ attenuates the frequency content for $\omega > \omega_g$ as $\omega \to \infty$, and amplifies the frequencies in the vicinity of $\omega = \omega_g$; the second filter $H_c(\omega)$ is then introduced to eliminate the low-frequency content, thus assuring finite power for the ground displacement.

Table 1 lists filter parameter values for producing reasonable spectral shapes for 'firm', 'medium' and 'soft' soils, as suggested in [26]. Figure 3 plots the corresponding curves for $S_0 = 1$, where the soft soil indicates a narrow-band process while the firm ground is broad-band with significant high frequency content.

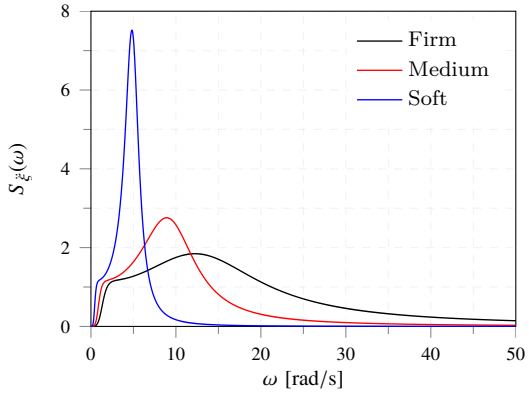

Figure 3: Clough-Penzien spectrum for different soil types [26].

Table 1: Filter parameters for different soil types [26].

Soil type	ω_g [rad/s]	ζ_g	ω_f [rad/s]	ζ_f
Firm	15.0	0.6	1.5	0.6
Medium	10.0	0.4	1.0	0.6
Soft	5.0	0.2	0.5	0.6

5 STEADY-STATE STATIONARY RESPONSE QUANTIFICATION

We next consider the case where the statistics of the steady-state, stationary response are of interest and the intensity of the base acceleration is sufficiently high such that the probability of sticking can be regarded negligible. In this case, the bottom part of Eq. (5) and (6) is valid for all time.

5.1 Fixed-base sliding block

Following the procedure delineated in [17] the nonlinear Eq. (2) is replaced with a linear one:

$$\ddot{u}_{\mathrm{s}}(t) = -\beta\,\dot{u}_{\mathrm{s}}(t) - \ddot{\xi}(t)\,, \tag{18}$$

where β represents a linear viscous damping term.

Minimising the mean square of the error $\varepsilon = \mu\,g\,\mathrm{sgn}\,(\dot{u}_{\mathrm{s}}(t)) - \beta\,\dot{u}_{\mathrm{s}}(t)$ with respect to β and after manipulation based on the standard assumption of zero mean Gaussian response, one obtains:

$$\beta = \left(\frac{2}{\pi}\right)^{\frac{1}{2}} \frac{\mu\,g}{\sigma_{\dot{u}_{\mathrm{s}}}}\,, \tag{19}$$

where $\sigma^2_{\dot{u}_{\mathrm{s}}} = \mathbb{E}\,\langle \dot{u}^2_{\mathrm{s}}(t)\rangle$ is the mean square of $\dot{u}_{\mathrm{s}}(t)$.

Further manipulation based on the specification of the spectrum, gives $\sigma_{u_{\mathrm{s}}}$ and $\sigma_{\dot{u}_{\mathrm{s}}}$ in terms of β:

$$\sigma^2_{u_{\mathrm{s}}} = \int_{-\infty}^{\infty} \left(\omega^2(\beta^2+\omega^2)\right)^{-1} S_{\ddot{\xi}}(\omega)\,\mathrm{d}\omega\,; \quad \sigma^2_{\dot{u}_{\mathrm{s}}} = \int_{-\infty}^{\infty} \left(\beta^2+\omega^2\right)^{-1} S_{\ddot{\xi}}(\omega)\,\mathrm{d}\omega\,. \tag{20}$$

Solution to Eq. (20) was presented in [17] for white noise excitation i.e. $S_{\ddot{\xi}}(\omega) = S_0$, in which case $\sigma^2_{\dot{u}_{\mathrm{s}}} = \pi S_0/\beta$ and $\beta = 2(\mu\,g)^2/\pi^2 S_0$. In the case where the excitation is characterised by the Kanai-Tajimi spectrum (i.e. setting $H_c(\omega) = 1$ in Eq. (16)), solution is reported in [16]. Notably, for both these cases, the first integral in Eq. (20) is infinite which implies that the mean-square of the displacement will indefinitely grow with time.

Further extending the existing contributions, we present here solutions for the Clough-Penzien spectrum in Eq. (16).

Analytical evaluation of Eq. (20) gives:

$$\sigma^2_{u_{\mathrm{s}}} = \frac{\pi S_0\,\omega_g^2(\mathcal{C}_1+\mathcal{C}_2)}{2\,\zeta_f\,\zeta_g\,\omega_f\,\mathcal{C}_3\,\mathcal{C}_4}\,; \quad \sigma^2_{\dot{u}_{\mathrm{s}}} = \frac{\pi S_0\,\omega_g^2(\mathcal{C}_5+\mathcal{C}_6)}{2\,\zeta_f\,\zeta_g\,\mathcal{C}_3\,\mathcal{C}_4}\,, \tag{21}$$

where the coefficients $\mathcal{C}_1$ - $\mathcal{C}_6$ are given by:

$$\mathcal{C}_1 = \beta\,(2\,\zeta_f\omega_f + 2\,\zeta_g\omega_g + \beta)\,\mathcal{C}_8\,; \tag{22a}$$
$$\mathcal{C}_2 = \omega_g\left(\omega_f^3\,\mathcal{C}_7 + \zeta_g\omega_g\left(4\omega_f^2\left(\zeta_f^2+\zeta_g^2\right) + 4\zeta_f\zeta_g\omega_f\omega_g + \omega_g^2\right)\right)\,; \tag{22b}$$
$$\mathcal{C}_3 = \left(\beta^2 + 2\beta\zeta_f\omega_f + \omega_f^2\right)\left(\beta^2 + 2\beta\zeta_g\omega_g + \omega_g^2\right)\,; \tag{22c}$$
$$\mathcal{C}_4 = 2\,\omega_f^2\omega_g^2\left(2\zeta_f^2 + 2\zeta_g^2 - 1\right) + 4\zeta_f\zeta_g\omega_f^3\omega_g + 4\zeta_f\zeta_g\omega_f\omega_g^3 + \omega_f^4 + \omega_g^4\,; \tag{22d}$$
$$\mathcal{C}_5 = \omega_g(2\beta(\zeta_f\omega_g + \zeta_g\omega_f) + \omega_f\omega_g)\,\mathcal{C}_8\,; \tag{22e}$$
$$\mathcal{C}_6 = \beta^2\left(\omega_g^3\,\mathcal{C}_7 + 4\zeta_g^3\left(4\zeta_f^2\omega_f\omega_g^2 + \omega_f^3\right) + 16\zeta_f\zeta_g^4\omega_f^2\omega_g + \zeta_g\omega_f\omega_g^2\right)\,, \tag{22f}$$

in which $\mathcal{C}_7 = \zeta_f\left(4\,\zeta_g^2 + 1\right)$ and $\mathcal{C}_8 = 4\,\zeta_g^3\omega_f^2 + \zeta_g\omega_g^2 + \zeta_f\left(4\zeta_g^2+1\right)\omega_f\,\omega_g$.

On combining Eq. (19) with Eq. (21), the resulting algebraic equation can be solved numerically for β and therefore σ_{u_s} and $\sigma_{\dot{u}_\mathrm{s}}$ can be evaluated from Eq. (21).

5.2 Base-isolated sliding block

The TDoF base-isolated block is next considered. The system is of chain-like structure and statistical linearisation is admissible. Accordingly, the term $\mathrm{sgn}\,(\dot{u}_\mathrm{s}(t))$ in Eq. (6), is replaced with the linear viscous damping term β, which assumes a similar form as the fixed-base block, except that $\sigma_{\dot{u}_\mathrm{s}^\mathrm{b}}$ (i.e. the standard deviation of $\dot{u}_\mathrm{s}^\mathrm{b}(t)$), is used in place of $\sigma_{\dot{u}_\mathrm{s}}$ in Eq. (19).

The equation of motion of the equivalent linear system then reads:

$$\ddot{u}_\mathrm{s}^\mathrm{b}(t) = \frac{-\beta\dot{u}_\mathrm{s}^\mathrm{b}(t) + 2\,\zeta\omega_\mathrm{b}\,\dot{u}_\mathrm{b}(t) + \omega_\mathrm{b}^2\,u_\mathrm{b}(t)}{1-\gamma}\,; \tag{23a}$$
$$\ddot{u}_\mathrm{b}(t) = \frac{\gamma\,\beta\dot{u}_\mathrm{s}^\mathrm{b}(t) - 2\,\zeta\omega_\mathrm{b}\,\dot{u}_\mathrm{b}(t) - \omega_\mathrm{b}^2\,u_\mathrm{b}(t)}{1-\gamma} - \ddot{\xi}(t)\,, \tag{23b}$$

where the spectral density matrix of the response process takes the form:

$$\mathbf{S}_u(\omega) = \mathbf{H}(\omega)\cdot\mathbf{S}_f(\omega)\cdot\mathbf{H}^{\top *}(\omega)\,, \tag{24}$$

in which $\mathbf{S}_f(\omega)$ denotes the spectral density matrix of the forcing, the symbols $\top$ and $*$ denote transposition and conjugation, respectively, and $\mathbf{H}(\omega)$ is the matrix of frequency response functions, given by:

$$\mathbf{H}(\omega) = \left[\begin{array}{c|c} \frac{\omega^2 - 2\,i\,\zeta\omega_\mathrm{b}\,\omega - \omega_\mathrm{b}^2}{\omega\,\mathbb{G}} & -\frac{\omega}{\mathbb{G}} \\ \hline -\frac{\gamma\,\omega}{\mathbb{G}} & \frac{\omega - \beta\,i}{\mathbb{G}} \end{array}\right]\,, \tag{25}$$

where $\mathbb{G}(\omega) = \omega^2((\gamma-1)\,\omega + i\,\beta) + 2\,\zeta\omega_\mathrm{b}(\beta + i\,\omega)\,\omega + \omega_\mathrm{b}^2(\omega - i\,\beta)$.

Further, the cross-variance of the response is evaluated through:

$$\mathbb{E}\,\langle u_i(t)u_j(t)\rangle = \int_{-\infty}^{\infty} S_{u_iu_j}(\omega)\,\mathrm{d}\omega\,; \quad \mathbb{E}\,\langle \dot{u}_i(t)\dot{u}_j(t)\rangle = \int_{-\infty}^{\infty}\omega^2 S_{u_iu_j}(\omega)\,\mathrm{d}\omega\,, \tag{26}$$

where $S_{u_iu_j}(\omega)$ is the (i,j)th element of $\mathbf{S}_u(\omega)$.

An alternative iterative procedure is employed for evaluating Eq. (26). Specifically, it is first assumed that $\beta = 0$ and the cross-variance terms in Eq. (26) are evaluated. These are used for determining a new estimate of β, which results in an update to Eq. (26). The procedure is repeated several times until accuracy is satisfactory.

6 NUMERICAL INVESTIGATIONS

The contributions presented in the preceding sections are next investigated by simulation techniques. Purpose is the quantification of the statistics of the steady-state stationary response of the systems under consideration due to filtered white noise excitation.

6.1 Piecewise linear solutions

The piecewise linear solutions presented in § 3 are first demonstrated on the nonlinear response quantification of fixed-base (FB) and base-isolated (IB) blocks with the purpose of assessing the validity of approximating the rigid-plastic behaviour with pure-sliding one (i.e. neglecting the rigid regime of motion, assuming that sliding is valid for all time). In the sequel, $u_{\mathrm{s}}(t)$ is used in place of $u_{\mathrm{s}}^{\mathrm{b}}(t)$, to represent the motion of the block relative to its base.

Figures 4(a) and 4(b) show two simulated realisations of the earthquake excitation, characterised by the Clough-Penzien power spectrum for a medium soil with $\omega_g = 10\,\mathrm{rad/s}$, $\zeta_g = 0.4$, $\omega_f = 1\,\mathrm{rad/s}$, $\zeta_f = 0.6$ and $S_0 = 0.0025\,\mathrm{m^2/s^3}$. Details on the procedure used for generating the excitation time series are provided in Appendix B.

The relative displacement and relative velocity response time histories of the FB and IB systems have been quantified next using the proposed piecewise linear solutions. Each system has been successively modelled with idealised rigid-plastic (R) and sliding (S) behaviour, and the isolation parameters $\gamma = 0.04$, $\omega_{\mathrm{b}} = 1.5\,\mathrm{rad/s}$ and $\zeta = 0.05$ have been assumed.

Figures 4(c) and 4(e) show the response due to the first realisation of the excitation with $\mu = 0.02$, indicating excellent agreement between the rigid-plastic and sliding solutions. Plotting the response histories for the second realisation in Figures 4(d) and 4(f), with $\mu = 0.06$, shows pronounced variations between the rigid-plastic and sliding solutions for both the two systems under consideration.

Overall, considering the probability of sticking negligible appears reasonable for low values of μ, or when the excitation is sufficiently high. Under these conditions, the approximation is admissible for use in the statistical linearisation procedure. In cases where these conditions are not met, such an approximation can be checked a priori. It is finally noted that demonstrating the validity of the piecewise linear solutions through comparisons with reference ones, falls outside the scope of this paper.

6.2 Statistical linearisation

The effectiveness of the statistical linearisation (SL) procedure described in § 5 is investigated next for the two systems under consideration.

Figure 5 compares the standard deviation of the relative velocity response determined using the SL procedure, with the nonstationary one numerically evaluated using the piecewise linear solutions via pertinent Monte Carlo (MC) simulation ($N = 200$ realisations), for various parameter combinations of ω_{b} and μ. The analysis has been carried out for a medium soil ($\omega_g = 10\,\mathrm{rad/s}$, $\zeta_g = 0.4$, $\omega_f = 1\,\mathrm{rad/s}$, $\zeta_f = 0.6$), and with parameters $S_0 = 0.003\,\mathrm{m^2/s^3}$, $\gamma = 0.04$, and $\zeta = 0.05$.

As shown, for the fixed-base block, the standard deviation of the velocity response reaches stationarity in very short time. Further, for $\mu = 0.01$ and $\mu = 0.03$, there is good agreement between the MC and SL, confirming the validity of the expressions derived in § 5.1. Interestingly, the accuracy of the SL approximation deteriorates at higher values of μ, as evidenced by the large deviation for $\mu = 0.05$. This is in agreement with investigations carried out in [16] using the Kanai-Tajimi power spectrum.

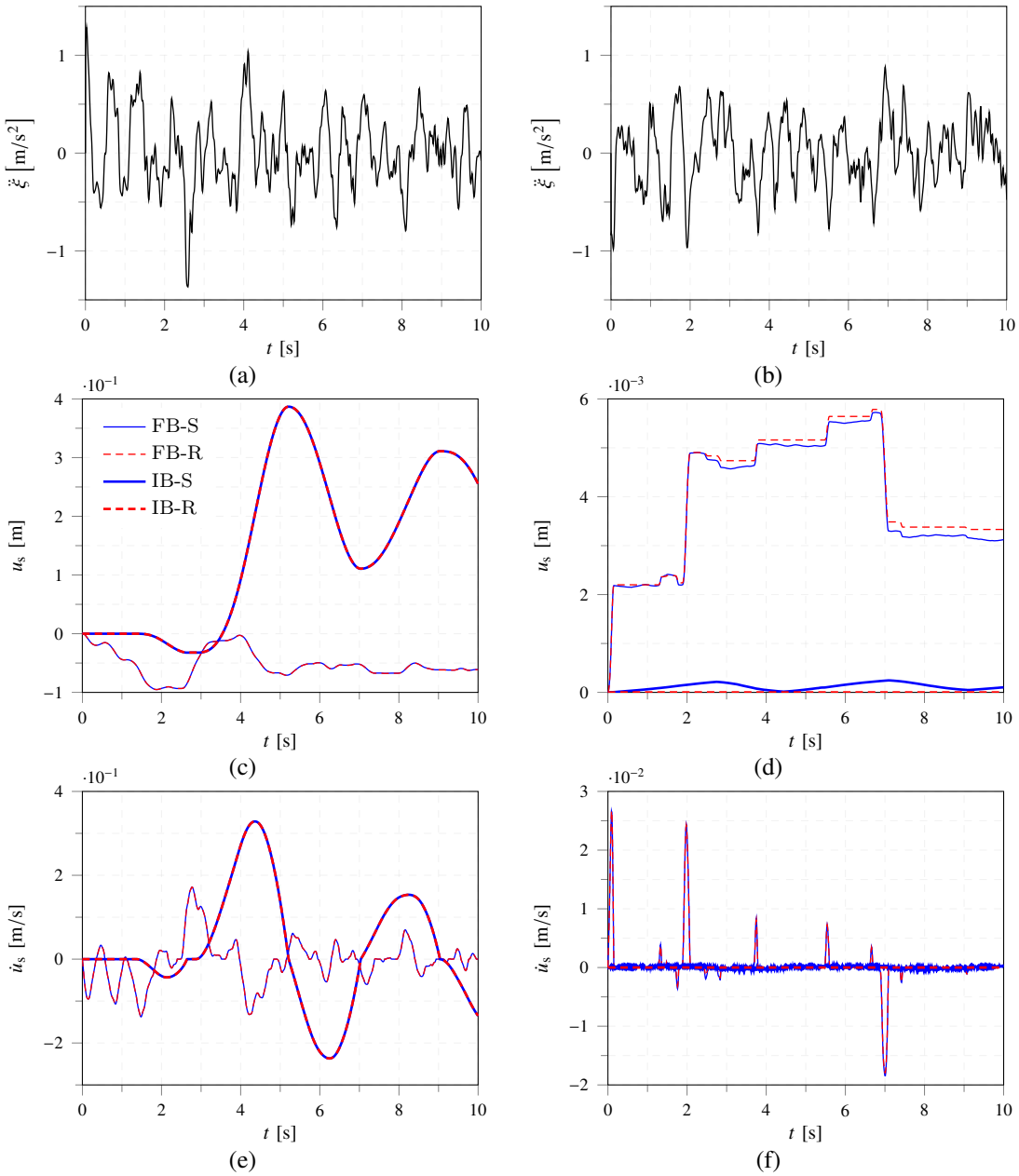

Figure 4: Response of fixed-base (FB) and base-isolated (IB) block, modelled with idealised rigid-plastic (R) and sliding (S) behaviour: realisations of base excitation (a, b) due to filtered white noise ($S_0 = 0.0025\,\mathrm{m^2/s^3}$, $\omega_g = 10\,\mathrm{rad/s}$, $\zeta_g = 0.4$, $\omega_f = 1\,\mathrm{rad/s}$, $\zeta_f = 0.6$); corresponding relative displacement and relative velocity response time histories ($\gamma = 0.04$, $\omega_\mathrm{b} = 1.5\,\mathrm{rad/s}$ and $\zeta = 0.05$) for $\mu = 0.02$ (c, d) and $\mu = 0.06$ (e, f).

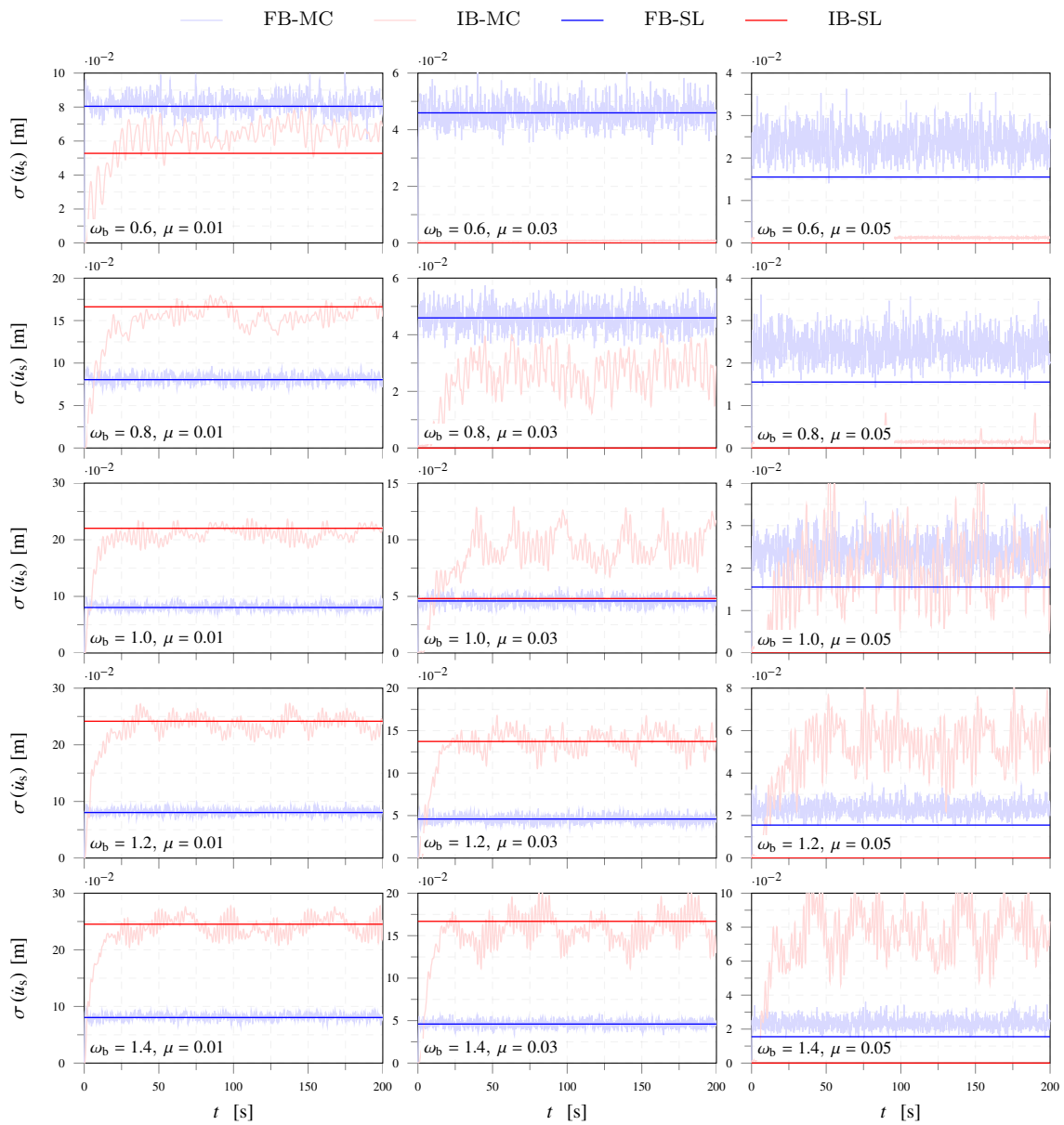

Figure 5: Standard deviation of relative velocity quantified for various parameter combinations of ω_b and μ: comparison of statistical linearisation (SL) and Monte Carlo (MC) simulation ($N = 200$ realisations), for the fixed-base (FB) and base-isolated (IB) block modelled with sliding behaviour. Reference parameters: $S_0 = 0.003\,\mathrm{m}^2/\mathrm{s}^3$; $\omega_g = 10\,\mathrm{rad/s}$, $\zeta_g = 0.4$, $\omega_f = 1\,\mathrm{rad/s}$, $\zeta_f = 0.6$ (medium soil); and $\gamma = 0.04$, $\zeta = 0.05$.

For the base-isolated block, the SL is found satisfactory for lower values of μ than those required for the fixed-base block, and for certain parameter combinations (e.g. $\omega_\mathrm{b} \geq 0.8$ and $\mu = 0.01$), while for other combinations (i.e. $\omega_\mathrm{b} = 0.8$ and $\mu = 0.03$) the iterative procedure employed for evaluating Eq. (26) does not converge and the solution breaks down. Further investigations are required to examine the influence of parameters γ and ζ on the effectiveness of the procedure.

6.3 Response spectra

A comparative study has been carried out with the purpose of assessing the effectiveness of the base isolation in suppressing the seismic forcing delivered to the block. Three soil types

have been considered, namely, firm ($\omega_g = 15\,\mathrm{rad/s}$, $\zeta_g = 0.6$, $\omega_f = 1.5\,\mathrm{rad/s}$, $\zeta_f = 0.6$); medium ($\omega_g = 10\,\mathrm{rad/s}$, $\zeta_g = 0.4$, $\omega_f = 1\,\mathrm{rad/s}$, $\zeta_f = 0.6$) and soft ($\omega_g = 5\,\mathrm{rad/s}$, $\zeta_g = 0.2$, $\omega_f = 0.5\,\mathrm{rad/s}$, $\zeta_f = 0.6$). In all cases, a spectral density level $S_0 = 0.003\,\mathrm{m^2/s^3}$ has been considered, and the isolation parameters $\gamma = 0.04$ and $\zeta = 0.05$ have been assumed.

For each case, an ensemble of $N = 200$ synthetic ground motions has been generated using the procedure delineated in Appendix B, and Monte Carlo simulations have been used to quantify the stationary value of the standard deviation of the velocity response of each system.

Figure 6 plots the calculated standard deviation of the response, for several values of the parameters ω_b, and μ, where the standard deviation of the response of the base-isolated block ($\sigma_\mathrm{IB}(\dot{u}_\mathrm{s})$), has been normalised with respect to the corresponding value of the fixed-base ($\sigma_\mathrm{FB}(\dot{u}_\mathrm{s})$) model.

As shown, seismic isolation can attenuate the velocity response of the sliding block in all cases considered. Reducing the isolation frequency ω_b results in a reduction in the response standard deviation, and as $\omega_\mathrm{b} \to \infty$, the response of the isolated block approaches the response of the fixed-base block (i.e. $\sigma_\mathrm{IB}/\sigma_\mathrm{FB} \to 1$). Seismic isolation is effective for $\omega_\mathrm{b} < 1.25$, $\omega_\mathrm{b} < 1$ and $\omega_\mathrm{b} < 0.7$, for the firm, medium and soil, respectively, and higher values of ω_b are admissible as μ increases.

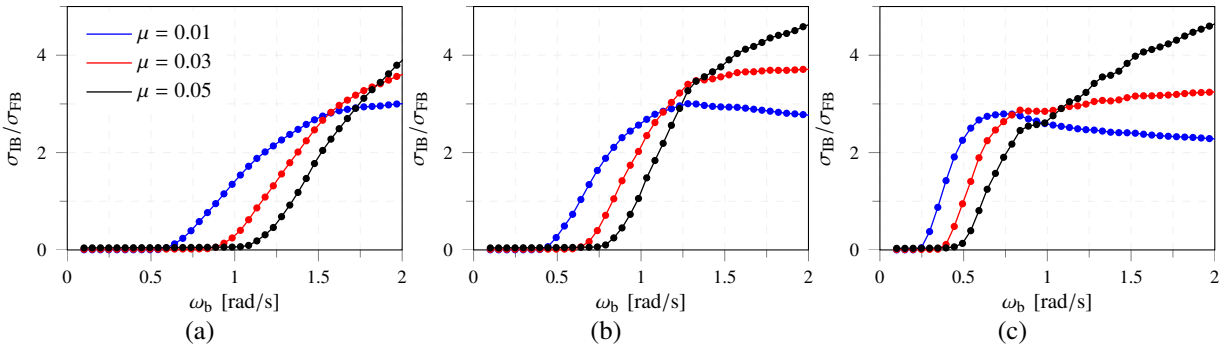

Figure 6: Isolated to non isolated standard deviation of relative velocity, quantified via $N = 200$ Monte Carlo realisations: (a) firm ($\omega_g = 15\,\mathrm{rad/s}$, $\zeta_g = 0.6$, $\omega_f = 1.5\,\mathrm{rad/s}$, $\zeta_f = 0.6$); (b) medium ($\omega_g = 10\,\mathrm{rad/s}$, $\zeta_g = 0.4$, $\omega_f = 1\,\mathrm{rad/s}$, $\zeta_f = 0.6$); and (c) soft ($\omega_g = 5\,\mathrm{rad/s}$, $\zeta_g = 0.2$, $\omega_f = 0.5\,\mathrm{rad/s}$, $\zeta_f = 0.6$) soil. Reference parameters: $S_0 = 0.003\,\mathrm{m^2/s^3}$, $\gamma = 0.04$ and $\zeta = 0.05$.

7 CONCLUSIONS

The modelling and response quantification of fixed-base and base-isolated rigid-plastic blocks were addressed in presence of stochastic forcing with indicative application to seismic engineering.

The dynamics of fixed-base rigid-plastic blocks were first overviewed, and equations governing their full dynamic interaction with a linear base-isolation system were presented. Highly-efficient piecewise numerical solutions were then derived for the two systems under consideration, which permit accurate quantification of the true nonlinear response due to a general-type excitation via pertinent Monte Carlo simulations.

A statistical linearisation approximation approach was adopted in view of approximating the strongly nonlinear systems during the sliding motion regime in presence of filtered white noise excitation, characterised by the Clough-Penzien stationary power spectrum, commonly used in earthquake engineering applications.

The accuracy of the linearisation approximation was examined and the effectiveness of the isolation system was assessed in attenuating the forcing delivered to the block.

The work delivers insights into the determination and understanding of the probabilistic characteristics of dynamically driven fixed-base and base-isolated rigid-plastic systems, motivating further investigations.

APPENDIX A. SOLVERS FOR THE SDOF AND TDOF NONLINEAR SYSTEMS

The piecewise linear solutions presented in § 3, govern the true nonlinear response of the systems considered and have been implemented in C++ resulting in standalone solver executable files. An iterative procedure based on the bisection method [27] has been adopted to identify state events (i.e. transition points such as the initiation and change in the regime of motion) and break down the solution in parts which have been later pieced together.

In order to confirm the validity of the solvers the solution has been compared to a MATLAB [28] implementation that has been prototyped using build-in Ordinary Differential Equation solvers. Specifically, ODE45 has been used, which is based on an explicit fourth- and fifth-order Runge-Kutta formulation. In this implementation, the continuous function $\tanh\left(\alpha\,\dot{u}_{\mathrm{s}}(t)\right)$ has been used in place of $\mathrm{sgn}\left(\dot{u}_{\mathrm{s}}(t)\right)$, where α is a large constant. Further, consistent initial conditions have been used, and MATLAB's odeset parameters have been set to AbsTol $=$ RelTol $=$ 10^{-8} and Refine $= 4$, which refer to relative and absolute solution tolerances and interpolation output, respectively. The option 'Events' has been invoked to identify state events.

APPENDIX B. SIMULATION OF STOCHASTIC FORCING

A stationary stochastic process representing the excitation time series ensemble, is generated through the summation of cosines with amplitudes and frequencies characterised by the power spectrum under consideration and random phases uniformly distributed over the interval $[0, 2\pi]$ [29]. In doing this, a frequency interval $[0, \tilde{\omega}]$ is considered, where $\tilde{\omega} = 100$ is an upper cut-off frequency, beyond which the spectral density is negligible. This interval is discretised using a frequency step $\Delta\omega = \tilde{\omega}/N_{\omega}$, where $N_{\omega} = \max\left\{N_0, \mathrm{ceil}\left(\frac{\tilde{\omega}\,T}{4\pi}\right)\right\}$ depends on $N_0 \approx 100$ (chosen such that the variance of the resulting process closely approximates the PSD) and on the temporal duration T of interest [30]. The time series is finally discretised using a time step $\Delta t \leq \frac{\pi}{4\,\tilde{\omega}}$.

References

[1] M. Riley, T. Coats, K. Haupt and D. Jacobson. Ride Severity Index - A new approach to quantifying the comparison of acceleration responses of high-speed craft. *11th International Conference on Fast Sea Transportation*, 2011.

[2] A. Malhotra and J. Penzien. Nondeterministic analysis of offshore structures. *Journal of the Engineering Mechanics Division*, **96**, 985–1003, 1970.

[3] S. Spence and M. Gioffre. Large scale reliability-based design optimization of wind excited tall buildings. *Probabilistic Engineering Mechanics*, **28**, 206–215, 2012.

[4] S. Kasinos. *Seismic response analysis of linear and nonlinear secondary structures*. PhD thesis, 2018.

[5] B. Westermo and F. Udwadia. Periodic response of a sliding oscillator system to harmonic excitation. *Earthquake Engineering and Structural Dynamics*, **11**, 135–146, 1983.

[6] N. Makris and M. Constantinou. Analysis of motion resisted by friction. I. Constant coulomb and linear/coulomb friction. *Mechanics of Structures and Machines*, **19**, 477–500, 1991.

[7] E. Voyagaki, G. Mylonakis and I. Psycharis. Rigid block sliding to idealized acceleration pulses. *Journal of Engineering Mechanics*, **138**, 1071–1083, 2012.

[8] E. Voyagaki, G. Mylonakis and I. Psycharis. A shift approach for the dynamic response of rigid-plastic systems. *Earthquake Engineering and Structural Dynamics*, **40**, 847–866, 2011.

[9] M. C. Constantinou, G. Gazetas and I. G. Tadjbakhsh. Stochastic seismic sliding of rigid mass supported through non-symmetric friction. *Earthquake Engineering and Structural Dynamics*, **12**, 777–793, 1984.

[10] K. Kanai. An empirical formula for the spectrum of strong earthquake motions. *Bulletin of the Earthquake Research Institute, University of Tokyo, Japan*, **39**, 1961.

[11] H. Tajimi. A statistical method of determining the maximum response of a building structure during an earthquake. *Proceedings of the 2nd World Conference in Earthquake Engineering*, 1960.

[12] S. Crandall, S. Lee and J. Williams. Accumulated slip of a friction-controlled mass excited by earthquake motions. *Journal of Applied Mechanics*, **41**, 1094–1098, 1974.

[13] S. Crandall and S. Lee. Biaxial slip of a mass on a foundation subject to earthquake motion. *Ingenieur-Archiv*, **45**, 361–370, 1976.

[14] G. Ahmadi. Stochastic Earthquake Response of Structures on Sliding Foundation. *International Journal of Engineering Science*, **21**, 93–102, 1983.

[15] T. Noguchi. The Response of a Building on Sliding Pads to Two Earthquake Models. *Journal of Sound and Vibration*, **103**, 437–442, 1985.

[16] M. C. Constantinou and I. G. Tadjbakhsh. Response of a sliding structure to filtered random excitation. *Journal of Structural Mechanics*, **12**, 401–418, 1984.

[17] J. Roberts and P. Spanos. *Random vibration and statistical linearisation*. Dover, 2003.

[18] I. Kougioumtzoglou and P. Spanos. Nonlinear MDOF system stochastic response determination via a dimension reduction approach. *Computers and Structures*, **126**, 135–148, 2013.

[19] J. Kelly. *Earthquake-resistant design with rubber*. Springer: London, 1997.

[20] B. Palazzo and L. Petti. Stochastic response comparison between base isolated and fixed-base structures. *Earthquake Spectra*, **13**, 77–96, 1997.

[21] F. Nikfar and D. Konstantinidis. Sliding response analysis of operational and functional components (OFC) in seismically isolated buildings. *3rd Specialty Conference on Disaster Prevention and Mitigation*, 2013.

[22] D. Konstantinidis and F. Nikfar. Seismic response of sliding equipment and contents in base-isolated buildings subjected to broadband ground motions. *Earthquake Engineering and Structural Dynamics*, **44**, 865–887, 2015.

[23] P. Roussis and S. Odysseos. Slide-rocking response of seismically-isolated rigid structures subjected to horizontal ground excitation. *2nd European Conference on Earthquake Engineering and Seismology*, 2014.

[24] H. Hong and S. Liu. Coulomb friction oscillator: modelling and responses to harmonic loads and base excitations. *Journal of Sound and Vibration*, **229**, 1171–1192, 2000.

[25] R. W. Clough and J. Penzien. *Dynamics of structures*. McGraw-Hill, 1975.

[26] A. Der Kiureghian and A. Neuenhofer. Response spectrum method for multi-support seismic excitations. *Earthquake Engineering and Structural Dynamics*, **21**, 713–740, 1992.

[27] K. Atkinson. *An introduction to numerical analysis*. John Wiley & Sons, 2008.

[28] The MathWorks Inc. MATLAB. *Release 8.2*, 2013.

[29] M. Shinozuka and G. Deodatis. Simulation of stochastic processes by spectral representation. *Applied Mechanics Reviews*, **44**, 191–204, 1991.

[30] G. Muscolino. *Dinamica delle strutture*. McGraw-Hill, 2001.